Munc18c Depletion Selectively Impairs the Sustained Phase of Insulin Release

Eunjin Oh and Debbie C. Thurmond

OBJECTIVE—The Sec1/Munc18 protein Munc18c has been implicated in Syntaxin 4–mediated exocytosis events, although its purpose in exocytosis has remained elusive. Given that Syntaxin 4 functions in the second phase of glucose-stimulated insulin secretion (GSIS), we hypothesized that Munc18c would also be required and sought insight into the possible mechanism(s) using the islet β-cell as a model system.

RESEARCH DESIGN AND METHODS—Perifusion analyses of isolated Munc18c- (−/+) or Munc18c-depleted (RNAi) mouse islets were used to assess biphasic secretion. Protein interaction studies used subcellular fractions and detergent lysates prepared from MIN6 β-cells to determine the mechanistic role of Munc18c in Syntaxin 4 activation and docking/fusion of vesicle-associated membrane protein (VAMP)2-containing insulin granules. Electron microscopy was used to gauge changes in granule localization.

RESULTS—Munc18c (−/+) islets secreted ~60% less insulin selectively during second-phase GSIS; RNAi-mediated Munc18c depletion functionally recapitulated this in wild-type and Munc18c (−/+) islets in a gene dosage-dependent manner. Munc18c depletion ablated the glucose-stimulated VAMP2–Syntaxin 4 association as well as Syntaxin 4 activation, correlating with the deficit in insulin release. Remarkably, Munc18c depletion resulted in aberrant granule localization to the plasma membrane in response to glucose stimulation, consistent with its selective effect on the second phase of secretion.

CONCLUSIONS—Collectively, these studies demonstrate an essential positive role for Munc18c in second-phase GSIS and suggest novel roles for Munc18c in granule localization to the plasma membrane as well as in triggering Syntaxin 4 accessibility to VAMP2 at a step preceding vesicle docking/fusion. ***Diabetes*** **58:1165–1174, 2009**

Numerous recent reports link type 2 diabetes with single-nucleotide polymorphisms (SNPs) and reduced abundance of exocytosis proteins such as soluable *N*-ethylmaleimide attachment protein receptor (SNARE) proteins and their regulatory Munc18 binding partners (1–4). Moreover, several animal models of insulin resistance and insulin secretory dysfunction lack normal levels of SNARE proteins (rev. in 5), and experimental induction of diabetes using streptozotocin results in loss of expression of SNARE proteins (6). In contrast, increasing amounts of select SNARE proteins leads to enhanced insulin sensitivity via increasing glucose uptake into skeletal muscle as well as enhancing insulin release in vivo (7,8) and has also been shown to restore normal insulin secretion in diabetic rodent models (9). However, alteration of the endogenous level of the regulatory protein Munc18c in either direction is implicated in disrupted glucose homeostasis and type 2 diabetes (4,10,11), indicating the need for mechanistic clarification of the role(s) of Munc18c in the exocytotic processes that govern the maintenance of whole-body glucose homeostasis.

Biphasic insulin release is believed to be important for optimal glucose homeostasis. The first phase of insulin release is well studied and known to be triggered by the entry and metabolism of glucose into the β-cell via the constitutively plasma membrane–localized GLUT2 transporter, leading to a net increase in intracellular ATP-to-ADP ratio (rev. in 12). This result induces closure of the ATP-dependent K^+ channels and membrane depolarization, upon which the voltage-dependent calcium channels open to promote calcium entry (13–15). Calcium entry triggers fusion of the insulin granules docked/primed in the readily releasable pool at the plasma membrane via Syntaxin 1A– and Syntaxin 4–dependent mechanisms (8,16,17). Immediately after the first phase comes a second and sustained phase of insulin release, which is attributed to the refilling of the readily releasable pool from more intracellular insulin granule storage pools (18). The mechanisms underlying biphasic insulin secretion have yet to be fully elucidated, although this biphasic pattern is now recognized as being conserved among human, rat, and mouse islets under short-term culture conditions (19–22).

Vesicle exocytosis involves the specific binding of the vesicle-associated membrane protein (VAMP) v-SNARE with a binary cognate receptor t-SNARE complex, composed of SNAP25/23 and Syntaxin proteins, to form the heterotrimeric SNARE core complex (rev. in 23). Plasma membrane–localized Syntaxin proteins are further regulated by SM proteins (Sec1/Munc18) that bind with selectivity to their cognate Syntaxins; Munc18a and Munc18b bind to Syntaxins 1–3, whereas only Munc18c binds to and regulates Syntaxin 4 in cells (24–27). All three Munc18 isoforms are expressed in islet β-cells, although only Munc18a and Munc18c have been implicated in insulin release to date (7,8,28). Munc18a RNAi-mediated depletion was used to establish its positive role in insulin secretion through Syntaxin 1 (28), with Syntaxin 1 recognized as key to first-phase insulin release but not for second-phase release (17). Similarly, islets isolated from Munc18c (−/+) knockout mice secrete significantly less insulin in response to glucose stimulation in static culture studies, contributing to the increased susceptibility of the Munc18c (−/+) knockout mice for developing type 2 diabetes (29).

From the Department of Biochemistry and Molecular Biology, Center for Diabetes Research, Indiana University School of Medicine, Indianapolis, Indiana.

Corresponding author: Debbie C. Thurmond, dthurmon@iupui.edu.

Received 1 August 2008 and accepted 26 January 2009.

Published ahead of print at http://diabetes.diabetesjournals.org on 2 February 2009. DOI: 10.2337/db08-1059.

Because Munc18c function has so far been linked to Syntaxin 4–mediated granule exocytosis and Syntaxin 4 has been shown to be required for both phases of insulin release (7,8), we hypothesized that Munc18c would function in at least one of the two phases of insulin release. In addition, Munc18 proteins have recently been implicated in binding events with nonsyntaxin proteins, suggesting that its role in biphasic insulin exocytosis could also be Syntaxin 4 independent.

In the present study, we investigated the functional and mechanistic roles of Munc18c in regulating glucose-stimulated biphasic insulin secretion. Islets isolated from Munc18c (−/+) heterozygous knockout mice were selectively deficient in second-phase insulin secretion; RNAi-mediated depletion of endogenous Munc18c in isolated islets fully recapitulated this defect. Multiple mechanistic defects associated with Munc18c depletion were revealed that may cumulatively account for the selective functional lapse in second-phase insulin release: *1*) Munc18c depletion resulted in decreased Syntaxin 4 accessibility to VAMP2, supporting a role for the plasma membrane pool of Munc18c in a predocking step involving Syntaxin 4 activation and/or granule capture; *2*) Munc18c depletion resulted in significantly fewer granules visibly juxtaposed to the plasma membrane in electron micrographs, suggesting for the first time that the cytosolic pool of Munc18c may be functionally required for mobilizing granules in response to glucose stimulation.

RESEARCH DESIGN AND METHODS

Materials. The rabbit polyclonal anti-Munc18c antibody was generated as described (30). The rabbit Syntaxin 4, mouse clathrin, mouse anti–green fluorescent protein (GFP), and mouse VAMP2 antibodies were purchased from Chemicon (Temecula, CA), BD Biosciences (Franklin Lakes, NJ), Clontech (Mountain View, CA), and Synaptic Systems (Gottingen, Germany), respectively. Mouse anti-insulin and mouse monoclonal (M2) Flag antibodies were obtained from Sigma (St. Louis, MO), and the anti-mouse Texas Red secondary antibody was purchased from Jackson ImmunoResearch Laboratories (West Grove, PA), respectively. The MIN6 cells were a gift from Dr. John Hutton (University of Colorado Health Sciences Center). The sensitive rat insulin radioimmunoassay kit was acquired from Linco Research (St. Charles, MO).

Plasmids. Four different pSilencer1.0-siMunc18c constructs were generated by insertion of annealed double-stranded complementary oligonucleotides encoding 19 nucleotides (nt) of mouse Munc18c, followed by a loop region (TTCAAGAGA) and the antisense of the 19 nt. The 19 nt sequences were as follows: (number 1) 5′-ACAGCCGTGTTCGATGACT-3′; (number 2) 5′-GCAGCGTATATATACTTCA-3′; (number 3) 5′-GCAGATCTCGAAGCAAGTA-3′; and (number 4) 5′-AGGATCGGTCTGCAGAAGA-3′. The pSilencer1.0 control construct (siCon) was generated similarly, using a 19 nt sequence (GCGCGCTTTGTAGGATTCG) that failed to recognize any other mammalian protein (31). Oligonucleotides were generated to encode *Apa*I and *Eco*RI sites at the 5′ and 3′ ends, respectively, for insertion into the pSilencer 1.0-U6 vector (Ambion). The siMunc18c-Ad adenovirus was generated by insertion of the number 2 siRNA double-stranded complementary oligonucleotide fragment into the 5′ *Afl*II and 3′ *Spe*I sites of the pMighty vector (Viraquest, North Liberty, IA). The siCon-Ad was generated similarly in the pMighty vector, as previously described (31). Each construct was linearized by restriction digestion with *Nde*I and packaged with enhanced GFP (EGFP) to enable visualization of infection efficiency.

Cell culture, transient transfection, adenoviral transduction, and insulin secretion. CHO-K1 cells were purchased from the American Type Culture Collection (Manassas, VA) and cultured in Ham's F-12 medium supplemented with 10% fetal bovine serum, 100 U/ml penicillin, 100 μg/ml streptomycin, and 292 μg/ml L-glutamine. At 50–70% confluence, cells were transfected with 40 μg DNA as previously described (32) to obtain ~70% efficiency. MIN6 β-cells were cultured as described previously (32) and transduced at multiplicities of infection (MOI) = 50–100 for 1 h, washed with PBS, and incubated in MIN6 medium for 48 h. Cells were then preincubated for 2 h in glucose-free modified Krebs ringer bicarbonate buffer (MKRBB): 5 mmol/l KCl, 120 mmol/l NaCl, 15 mmol/l HEPES, pH 7.4, 24 mmol/l $NaHCO_3$, 1 mmol/l $MgCl_2$, 2 mmol/l $CaCl_2$ and 1 mg/ml BSA, stimulated with 20 mmol/l glucose for 30 min and buffer collected for quantitation of insulin released. Detergent cell lysates were prepared by harvesting in 1% Nonidet P-40 lysis buffer (1% NP-40, 25 mmol/l HEPES, pH 7.4, 10% glycerol, 50 μmol/l sodium fluoride, 10 mmol/l sodium pyrophosphate, 1 mmol/l sodium vanadate, 137 mmol/l sodium chloride, 1 mmol/l phenylmethylsulfonyl fluoride, 1 μg/ml pepstatin, and 10 μg/ml aprotinin) and lysates cleared by microcentrifugation for 10 min at 4°C for use in immunoprecipitation and immunoblotting. Subcellular fractions were isolated as previously described (33). All pellets were resuspended in the 1% NP-40 lysis buffer to ensure solubilization of membrane proteins.

Recombinant proteins and interaction assays. The GST-VAMP2 protein (soluble, TM domain deleted) was generated in *Escherichia coli* and purified by glutathione-agarose affinity chromatography as described previously (34) for use in the Syntaxin accessibility assay. GST-VAMP2 linked to sepharose beads was combined with 2 mg detergent cell lysate for 2 h at 4°C in NP-40 lysis buffer, followed by three stringent washes with lysis buffer, and associated proteins were resolved on 12% SDS-PAGE followed by transfer to polyvinylidene difluoride membrane for immunoblotting.

Mouse islet isolation and perifusion. All studies involving mice followed the guidelines for the use and care of laboratory animals at the Indiana University School of Medicine. Munc18c heterozygous (−/+) knockout mice have been described previously (29). All wild-type and Munc18c (−/+) male mice used in these studies were bred by HET×HET crosses from mice enriched on the C57BL/6J background to at least F16 and littermates used in paired islet isolations (−/− fail to survive beyond E7.5). Pancreatic mouse islets were isolated as previously described (8), with pancreata of five mice combined to generate each batch of islets. Islets were perifused at a flow rate of 0.3 ml/min for 10 min in KRB HEPES (KRBH) containing 2.8 mmol/l glucose with eluted fractions captured at 1-min intervals, followed by glucose stimulation (20 mmol/l) for 35 min. Quantitation of area under the curve for first- and second-phase insulin release was performed according to previously published criteria (35).

Adenoviral transduction of islets. Islets were isolated and immediately transduced at an MOI = 100 (based on assumption of 1,000 cells within each islet) with either siCon-Ad or siMunc18c-Ad CsCl-purified particles titered at 3×10^{10} and 1×10^{10} pfu/ml, respectively, for 1 h at 37°C in RPMI-1640. Transduced islets were then washed twice and incubated for 40 h at 37°C/5% CO_2. EGFP fluorescence was visualized in >95% of outer cells of islets in all experiments, and similarly fluorescent islets were handpicked for perifusion analysis.

Co-immunoprecipitation and immunoblotting. For each immunoprecipitation, 2 mg cleared detergent lysates were combined with 2 μg of indicated antibodies and allowed to rotate for 2 h at 4°C. Protein G Plus agarose beads were added and reactions rotated at 4°C for an additional 2 h. After three washes with lysis buffer, the resulting immunoprecipitates were subjected to 12% SDS-PAGE followed by transfer to polyvinylidene difluoride membrane for immunoblotting and bands visualized by enhanced chemiluminescence using a Chemi-Doc imaging system (Bio-Rad).

Electron microscopy. MIN6 β-cells were grown to ~80% confluence on Thermonox coverslips. Cells were incubated for 2 h in freshly prepared MKRBB buffer followed by stimulation with 20 mmol/l glucose for 5 min. Cells were fixed in a 0.1 mol/l cacodylate-buffered mixture of 2% glutaraldehyde and 2% paraformaldehyde for 30 min at room temperature followed by overnight incubation at 4°C and then postfixed in 1% OsO_4 for 1 h. En bloc staining in 0.5% aqueous uranyl acetate was performed for 3 h followed by a 10-min water wash. Dehydration was done in the following sequence: 50% ethanol, 70% ethanol, 95% ethanol, and 100% ethanol each for 10 min. Infiltration entailed ethanol and resin in the order of 3:1 (1 h), 1:1 (overnight), 1:3 (1 h), and 100% resin (two to three changes each 30 min). The Thermonox coverslips were inverted over a 1.5-ml centrifuge tube filled with resin and polymerized for 48 h at 60°C. Thin (60–100 nm) sections were cut using the microtome (Leica Ultracut). The thin sections were stained with uranyl acetate and lead citrate and viewed on the FEI Tecnai G2 Biotwin.

mRNA extraction and quantitative real-time PCR analysis. mRNA from islets was prepared using Trizol reagent (Invitrogen). mRNA was quantified by absorbance at 260 and 280 nm. Reverse transcription was performed using the Invitrogen SuperScript one-step RT-PCR kit and was done at 50°C for 50 min. The mRNA level was determined using the fluorescent intercalating dye SYBR-Green kit and the LightCycler system (RocheApplied Science, Indianapolis, IN). RNA (2 μg) was used for first-strand cDNA synthesis. Primer sequences for Munc18c were as follows: Munc18c sense, 5′- GGACCTG-GCACTTGGAACAG-3′; and antisense, 5′-GAGGAGCACCAGCATGGAGT-3′. Glyceraldehyde 3-phosphatase dehydrogenase (GAPDH) was used as an internal control. The cycle threshold (C_t) value, defined as the PCR cycle at which a statistically significant increase of reporter fluorescence is first detected, was used as a measure for the starting copy numbers of target genes. The ratio of the C_t value of Munc18c mRNA to that of GAPDH in islets was determined as the relative Munc18c mRNA level.

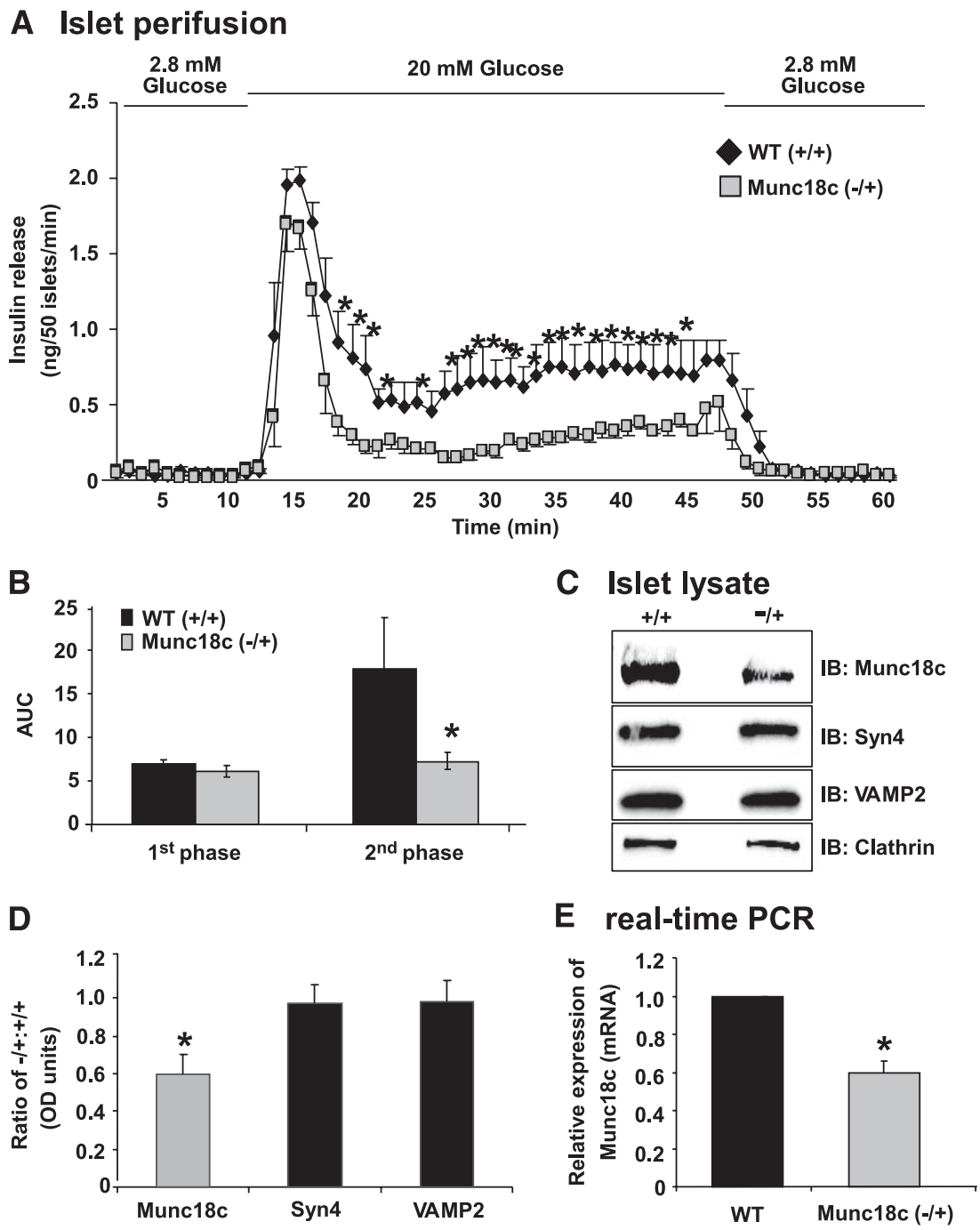

FIG. 1. Islets from Munc18c (−/+) mice have significantly impaired second-phase insulin secretion. Islets isolated from wild-type (WT) or Munc18c (−/+) mice were handpicked into groups of 50 and layered onto cytodex bead columns for parallel perifusion analysis. *A*: Islets were first preincubated for 30 min in low glucose (2.8 mmol/l), followed by basal sample collection (1–10 min) at low glucose to establish a baseline. Glucose was then elevated to 20 mmol/l for 35 min and subsequently returned to low glucose for 15 min. Eluted fractions were collected at 1-min intervals at a flow rate of 0.3 ml/min and insulin secretion was determined by radioimmunoassay. *B*: Quantitation of the area under the curve (AUC) for first-phase (11–17 min) and second-phase (18–45 min) insulin secretion from islets isolated from WT and Munc18c (−/+), normalized to baseline as described previously (8,35). *C*: Approximately 150 islets were solubilized in SDS sample buffer and resolved on 12% SDS-PAGE for immunoblotting (IB). *D*: Optical density scanning quantitation was used to derive the band density for each WT band, which was used to normalize that of Munc18c (−/+) bands in each experiment, and all bands were normalized to Clathrin. Data shown are the average ± SE of three to four independent sets of islets (*$P < 0.05$). *E*: Munc18c mRNAs from islets of WT (+/+) or Munc18c (−/+) mice were quantitated using real-time PCR. All Munc18c mRNA levels were normalized to GAPDH. Data represent the mean ± SE of three independent sets of islets (*$P < 0.05$).

Statistical analysis. All data were evaluated for statistical significance using Student's *t* test. Data are expressed as the mean ± SE.

RESULTS

Islets from Munc18c (−/+) knockout mice exhibit impaired second-phase insulin secretion. Islets were isolated from Munc18c (−/+) or wild-type littermate mice and perifused to measure insulin secretion every minute over a 60-min time period to determine which phase of glucose-stimulated insulin secretion (GSIS) required Munc18c (Fig. 1*A*). After an equilibration period of 30 min, islets were perifused for 10 min in KRBH buffer containing 2.8 mmol/l glucose to establish baseline secretion (basal), followed by stimulation for 35 min with 20 mmol/l glucose,

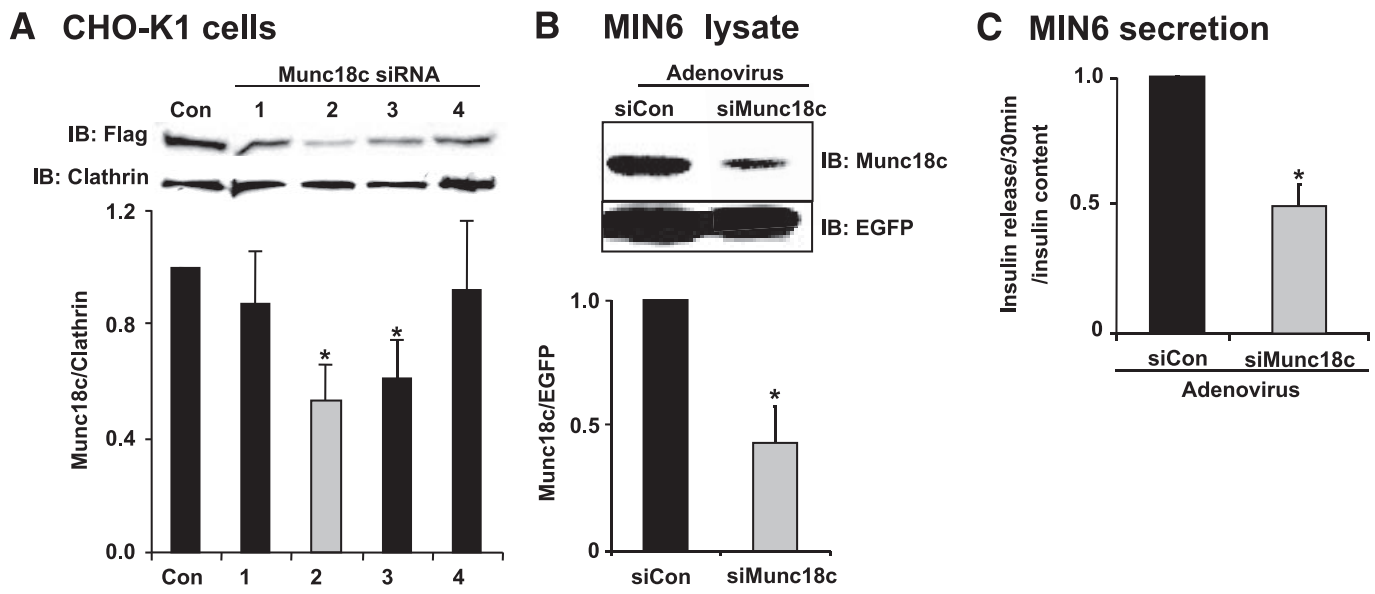

FIG. 2. RNAi-mediated Munc18c depletion recapitulates the loss of function observed in Munc18c (−/+) islets. *A*: Four Munc18c shRNA constructs and a noncoding control construct were each co-electroporated with pcDNA3-flag-Munc18c into CHO-K1 cells and detergent cell lysates prepared 48 h later to determine the efficiency of protein depletion achieved by each. Lysates were subjected to 10% SDS-PAGE for immunoblotting with anti-Flag and anti-clathrin (loading control) antibodies. Optical density scanning quantitation was used to derive the band density for each clathrin band, which was used to normalize that of Flag (Munc18c) bands in each experiment, and the mean ± SE of at least four independent sets of islets were determined (*$P < 0.05$). *B*: MIN6 cells transduced with siCon or siMunc18c adenoviruses, and after a 48-h incubation, cell lysates were prepared for use in anti-Munc18c immunoprecipitation and immunoblotting to detect knockdown efficiency. Anti-EGFP immunoblotting was used to indicate transduction efficiency and for normalization of Munc18c band densities in greater than three independent experiments (*$P < 0.05$). *C*: After a 48-h incubation following transduction by adenovirus, MIN6 cells were preincubated in MKRBB for 2 h and either left unstimulated or were stimulated with 20 mmol/l glucose for 30 min. Secreted insulin was measured by radioimmunoassay. Data shown are the means ± SE from three independent experiments (*$P < 0.05$).

and finally returned to basal conditions for an additional 15 min. Wild-type islets exhibited a peak within 5 min of glucose stimulation, consistent with the occurrence of first-phase insulin secretion. The first peak was followed by a sustained second phase that persisted at a level greater than threefold above basal level until glucose levels were reduced back to basal, mimicking insulin release kinetics previously reported (8,17,19,35). However, islets from Munc18c (−/+) mice secreted ~60% less during the second phase, as seen in three independent batches of perifused islets and quantitated by the area under the curve analysis according to established criteria (35), wherein the first phase occurs between minutes 11 and 17 and the second phase occurs between minutes 18 and 45 of the perifusion experiment (Fig. 1*B*). The Munc18c protein level in islets isolated from Munc18c (−/+) was reduced by at least 40% compared with wild-type islets (Fig. 1*C* and *D*), consistent with our previous observations using whole pancreas tissue extracts (29); abundances of Syntaxin 4 (Syn4) and VAMP2 were unchanged (Fig. 1*C* and *D*). Quantitative real-time PCR using RNA prepared from islets showed a specific loss of ~40% Munc18c mRNA compared with wild type (Fig. 1*E*; $P < 0.05$). These data expanded upon previous static incubation results by showing a selective and essential role for Munc18c in the second phase of GSIS.

RNAi-mediated depletion of Munc18c recapitulates the impaired insulin exocytosis phenotype of the Munc18c (−/+) mouse islets. RNAi-mediated depletion was used as an independent approach to assess the involvement of Munc18c in insulin secretion. Four different siRNA constructs were initially generated against Munc18c and introduced into Chinese hamster ovary (CHO)-K1 cells using a transient plasmid delivery system (pSilencer1.0-U6). Because the endogenous Munc18c protein was undetectable by the anti-Munc18c antibody in CHO-K1 cells, cells were co-electroporated with Flag-tagged recombinant Munc18c DNA plus one of the four different siRNA constructs to examine the capability of each siRNA to specifically deplete recombinant Munc18c protein expression compared with a control siRNA sequence (siCon). As seen in Fig. 2*A*, construct number 2 exerted the greatest reduction (~50%), and this siRNA was subsequently used in an adenoviral expression system to transduce MIN6 β-cells and isolated islets. The efficiency of endogenous siMunc18c-Ad depletion from MIN6 cells was 55% overall (Fig. 2*B*), and analysis of Munc18c depletion in plasma membrane and cytosolic fractions showed ~50% reduction of Munc18c protein each (data not shown). This loss of Munc18c protein corresponded to a 50% reduction in insulin release after a 30-min stimulation with glucose compared with GSIS from siCon-Ad cells (Fig. 2*C*). siMunc18c-Ad affected only glucose-stimulated release (625 ± 84 ng/ml for siCon vs. 340 ± 20 ng/ml for siMunc18c, $n = 3$), having no significant impact on basal insulin release (129 ± 14 ng/ml for siCon vs. 138 ± 11 ng/ml for siMunc18c, $n = 3$) or cellular insulin content (46,070 ± 2,510 ng/ml for siCon vs. 43,780 ± 2,000 ng/ml for siMunc18c, $n = 3$).

In islet perifusion analyses, wild-type islets transduced with siMunc18c-Ad exhibited significant reduction of second-phase GSIS compared with siCon-Ad islets, whereas first-phase secretion failed to show a statistically significant reduction (Fig. 3*A* and *B*). These data validate those results from our Munc18c (−/+) islets, supporting an important positive role for the Munc18c protein in second-phase insulin granule exocytosis. This validation of our Munc18c (−/+) mouse is important given the conflicting exocytosis results obtained using mouse embryonic fibro-

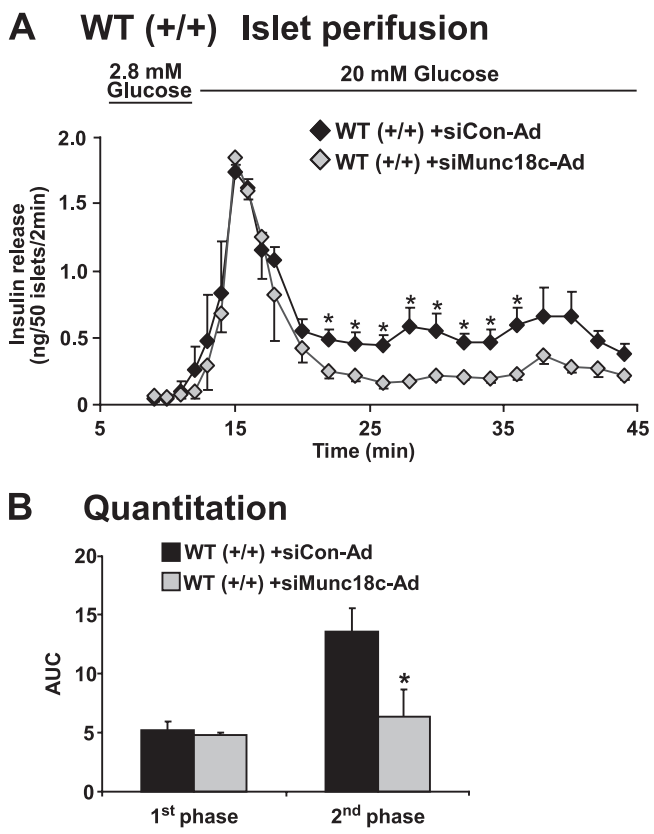

FIG. 3. RNAi-mediated depletion of Munc18c from MIN6 cells inhibits glucose-stimulated insulin release. *A*: Islets freshly isolated from wild-type (WT) mice were immediately transduced with siCon-Ad or siMunc18c-Ad adenovirus for 1 h, after which islets were washed and incubated for 40 h in RPMI medium. Evenly transduced GFP$^+$ islets were handpicked under a fluorescence microscope into groups of 50 and layered onto cytodex bead columns for paired (siCon versus siMunc18c) perifusion analyses, as described in Fig. 1. Data represent the mean ± SE for three independent perifusion studies using different islet preparations (*$P < 0.05$). *B*: Quantitation of the area under the curve (AUC) for first-phase (11–17 min) and second-phase (18–45 min) insulin secretion from WT islets transduced with siCon-Ad and siMunc18c-Ad. Data represent the mean ± SE for three independent experiments (*$P < 0.05$).

blasts derived from a different Munc18c knockout model (36).

To determine if the lack of effect upon first-phase insulin release was due to the heterozygosity of the islets and mere ~40–50% reduction of Munc18c protein, the abundance of Munc18c was further decreased by using siMunc18c-Ad to deplete Munc18c (−/+) islets. From siMunc18c-transduced Munc18c (−/+) islets, Munc18c protein expression was reduced by an additional 55% compared with levels present in the siCon-transduced Munc18c (−/+) islets (Fig. 4*A* and *B*), cumulatively reducing the endogenous Munc18c protein content by ~75% compared with wild-type islet Munc18c protein content. Syntaxin 4 and VAMP2 levels were unaffected by siMunc18c-Ad transduction (Fig. 4*B*). When subjected to islet perifusion analysis, siMunc18c-transduced Munc18c (−/+) islets exhibited a significant reduction in second-phase GSIS compared with siCon-transduced Munc18c (−/+) islets (Fig. 4*C* and *D*) or wild-type islets (red trace). Comparison of area under the curve calculated as representing first-phase secretion among wild-type (7.0 ± 0.3) nontransduced Munc18c (−/+) islets (6.0 ± 0.6), siCon-Ad–transduced Munc18c (−/+) islets (6.6 ± 0.6), and siMunc18c-Ad–transduced Munc18c (−/+) islets (5.3 ± 0.7) showed a small effect of Munc18c dosage as well ($P < 0.05$, wild-type vs. siMunc18c-Ad–transduced Munc18c (−/+) islets), albeit the more dramatic defect appeared to be in the second phase.

Munc18c depletion reduces the number of insulin granules localized to the plasma membrane. The reduction of second-phase GSIS from Munc18c (−/+)- or siMunc18c-transduced islets could result from impairment in one or multiple steps involved: granule mobilization from internal storage pools to the cell surface, granule docking/priming, or fusion of the granules with the plasma membrane. To discriminate between these possible steps, we began by assessing granule locale by electron microscopy within MIN6 cells transduced with siCon-Ad or siMunc18c-Ad. Because of the paucity of material obtainable from primary islet cells, MIN6 cells were used as a model system for mechanistic studies because they fully recapitulated the requirement for Munc18c in GSIS and are considered to be one of the clonal lines that has retained some level of biphasic secretion. Granule location with respect to distance from the plasma membrane was tabulated for each condition (siCon versus siMunc18c under basal and glucose-stimulated conditions) and grouped into one of three categories: localized within 50 nm, between 50 and 300 nm, or >300 nm from the plasma membrane. Granules located in the <50-nm group have been termed "morphologically docked" in the literature (18). Criteria for counting included the visualization of viral particles as confirmation of transduction and presence of the plasma membrane and of the nucleus in each field. Granule mobilization to the plasma membrane in MIN6 cells becomes evident as early as 5 min after glucose stimulation (34), consistent with the reported onset of a second phase beginning after 6 min in this cell line and also with the concept that mobilization events must begin during the first phase to sustain secretion. As shown in Fig. 5*A*, granules juxtaposed to the plasma membrane were clearly visible in the siCon-transduced cells that had been stimulated with glucose for 5 min compared with unstimulated/basal (Fig. 5*A*, *panels 1* and *2*); this was similar in micrographs prepared from cells stimulated for either 5 or 30 min (Fig. 5*A*, *panels 2* and *3*). In contrast, glucose-stimulated siMunc18c-Ad–transduced cells contained significantly fewer granules within the 50-nm range (Fig. 5*A*, *panels 5* and *6*, and *B*), although the total number of granules within each field of siCon-Ad and siMunc18c-Ad cells was similar (Fig. 5*C*). Analysis of granules in the more distant categories showed that in siMunc18c-Ad cells, a significant proportion of total granules remained >300 nm from the plasma membrane, even after glucose stimulation. Interestingly, there were no observable differences in granule proximity to the plasma membrane in unstimulated siCon-Ad or siMunc18c-Ad cells (Fig. 5*A*, *panel 1* vs. *4*, and *B*). These data suggested that glucose-induced granule movement toward the plasma membrane in Munc18c-depleted cells was reduced and could represent a mechanism by which to explain the deficit in second-phase GSIS.

Munc18c depletion disrupts Syntaxin 4's activation and association with VAMP2. The reduction in granule number in close proximity to the plasma membrane in glucose-stimulated siMunc18c-transduced cells could have resulted from a failure of the granules to be retained at the plasma membrane via docking with Syntaxin 4 and/or of their failure to progress toward the plasma membrane. To test the first possibility, that Munc18c depletion impaired

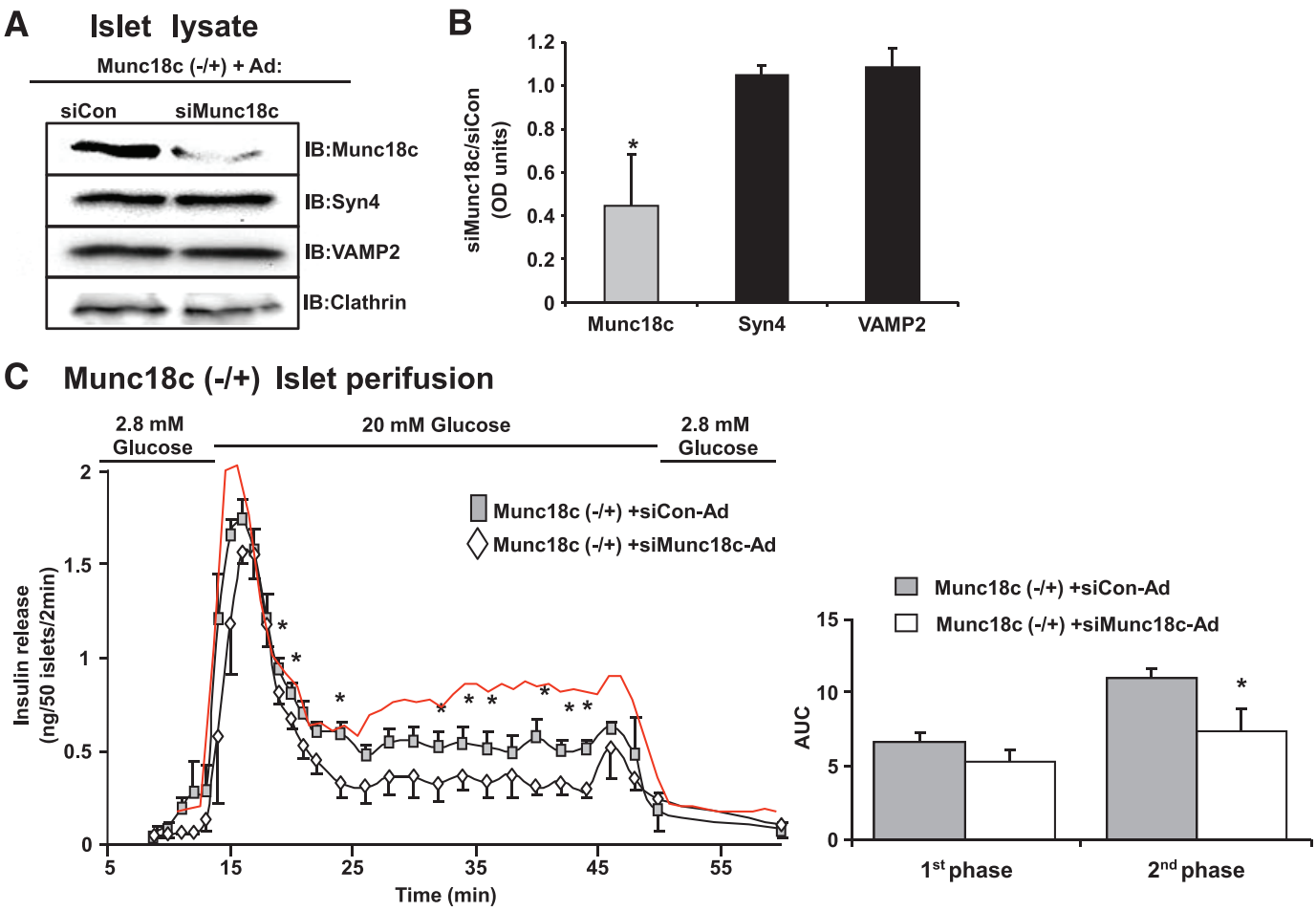

FIG. 4. Dose-dependent depletion of Munc18c corresponds to graded reduction of second-phase insulin release. Islets were isolated from Munc18c (−/+) mice and immediately transduced at MOI = 100 with siCon-Ad or siMunc18c-Ad for 1 h at 37°C. Islets were cultured for 40 h, after which GFP-expressing islets were handpicked under a fluorescent microscope for Western blot analysis (*A*) and optical density scanning thereof to determine level of knockdown (*B*), and for perifusion analysis (*C*), as described previously in Fig. 1*A*. Data represent the mean ± SE of three independent perifusion studies using different islet preparations (P* < 0.05). A trace from wild-type islets (*red line*) transduced with siCon-Ad is shown for comparison purposes. Quantitation of the area under the curve (AUC) for first-phase (11–17 min) and second-phase (18–45 min) insulin secretion from islets transduced with siCon-Ad and siMunc18c-Ad, normalized to baseline, is shown. Data represent the mean ± SE for three independent experiments (**P* < 0.05 vs. siCon-Ad). IB, immunoblotting. (A high-quality digital representation of this figure is available in the online issue.)**

docking/fusion of VAMP2-bound insulin granules with Syntaxin 4 at the plasma membrane, MIN6 cells were adenovirally transduced and detergent lysates of plasma membrane fractions (Fig. 6*A*) or cleared detergent cell lysates (Fig. 6*B*) prepared there from were used in anti–Syntaxin 4 immunoprecipitation reactions. Glucose stimulated a 1.8-fold increase in VAMP2 association with Syntaxin 4 in plasma membrane fractions prepared from siCon cells (Fig. 6*A*); no increase was seen in fractions from siMunc18c cells. Anti–Syntaxin 4 co-immunoprecipitated ~50% less Munc18c protein from siMunc18c-Ad plasma membrane fractions, consistent with the ~50% reduction of Munc18c protein from the plasma membrane compartment. Similar results were obtained using cleared detergent cell lysates prepared from siCon-Ad– or siMunc18c-Ad–transduced MIN6 cells (Fig. 6*B*); the glucose-stimulated increase in VAMP2–Syntaxin 4 association was only observed in siCon-treated lysates and not in siMunc18c-treated lysates (Fig. 6*B*). These data supported the notion that Munc18c was necessary for the glucose-induced steps at the plasma membrane that precede docking and/or fusion, although this assay cannot distinguish between effects upon docking (*trans*-SNARE complexes) versus fusion (*cis*-SNARE complexes).

To distinguish whether Munc18c was required to facilitate a glucose-induced increase in the Syntaxin 4 accessibility to VAMP2 docking, exogenous GST-VAMP2 (soluble form) protein linked to sepharose beads was added to cleared detergent cell lysates to "probe" for accessible Syntaxin 4, i.e., Syntaxin 4 that was available for binding. From siCon-transduced MIN6 cells stimulated with glucose, the GST-VAMP2 was able to co-precipitate significantly more Syntaxin 4 protein compared with that from unstimulated cells (Fig. 7*A* and *B*). In contrast, siMunc18c–transduced cell lysates lacked this glucose-stimulated increase in Syntaxin 4 association with GST-VAMP2. Syntaxin 4 immunoblotting of lysate input indicated lack of effect of siRNA adenoviral expression or of glucose treatment upon Syntaxin 4 protein abundance (Fig. 7*A*, *lanes 1–4*). Anti-GST immunoblotting indicated that equal levels of GST-VAMP2 protein were precipitated (Fig. 7*A*, *lanes 5–8*). Thus, these results suggested that Munc18c played an essential role in transitioning Syntaxin 4 into a more accessible conformation for its subsequent docking with VAMP2 in response to the glucose stimulus.

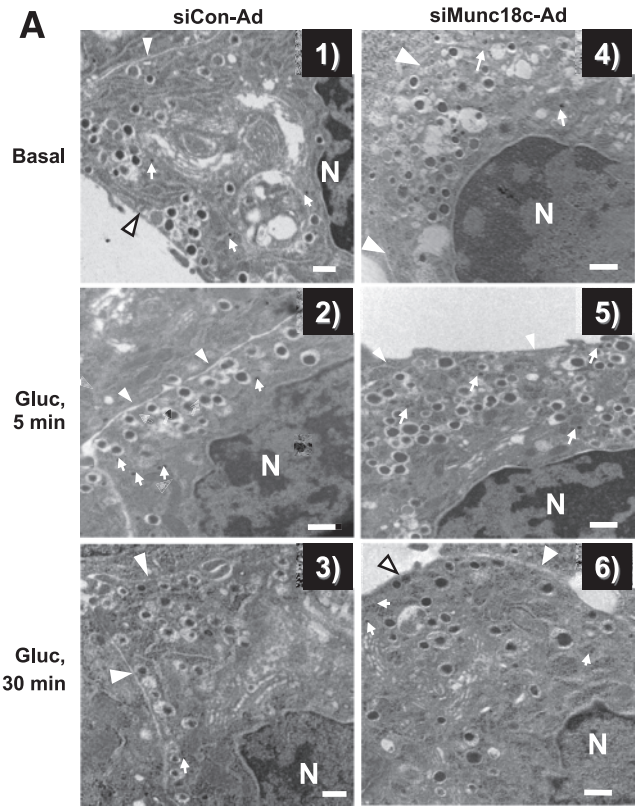

FIG. 5. Munc18c depletion alters insulin granule distribution. *A*: Transmission electron microscopy of MIN6 cells transduced with siCon-Ad (*panels 1–3*) or siMunc18c-Ad (*panels 4–6*) adenoviral particles. Cells were incubated for 48 h and then placed in glucose-free MKRBB for 2 h and subsequently stimulated with 20 mmol/l glucose (Gluc) for 5 min (*panels 2* and *5*) or 30 min (*panels 3* and *6*), or left unstimulated (basal, *panels 1* and *4*) and fixed for electron microscopy as described in RESEARCH DESIGN AND METHODS. Arrows indicate the presence of viral particles; arrowheads denote the plasma membrane. Bar = 500 nm. *B*: Distribution of insulin granules in siCon-Ad– and siMunc18c-Ad–transduced cells. Criteria for inclusion were presence of viral particles, clear demarcation of the plasma membrane, and presence of nucleus in each field tabulated. Insulin granule distance from the plasma membrane was tabulated for siCon and siMunc18c electron micrographs from 48 randomly selected MIN6 cells, with a total of 1,063 granule distances measured and grouped into categories based on the distance from the plasma membrane (*$P < 0.05$ vs. siCon-Ad). *C*: Total granule number per field/section in siCon-Ad–and siMunc18c-Ad–transduced cells under each condition was quantified.

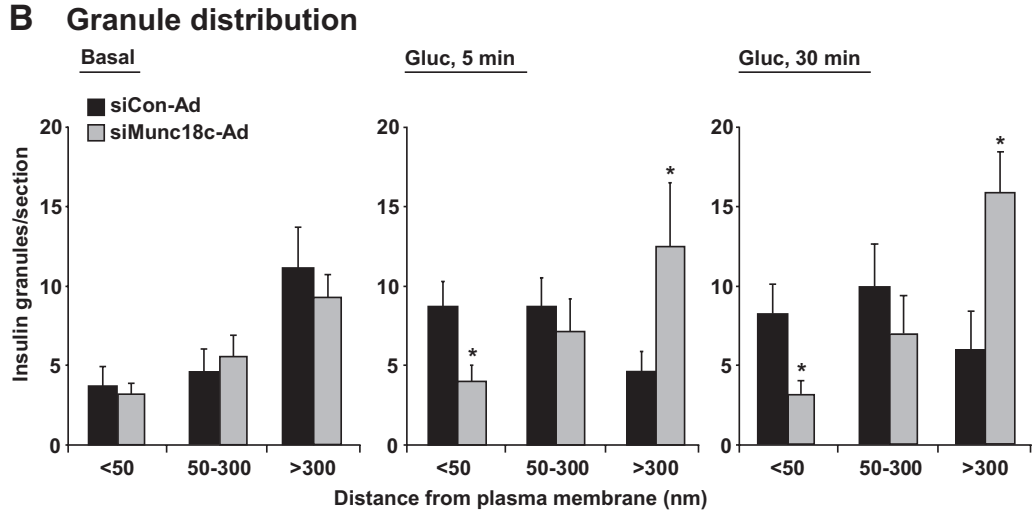

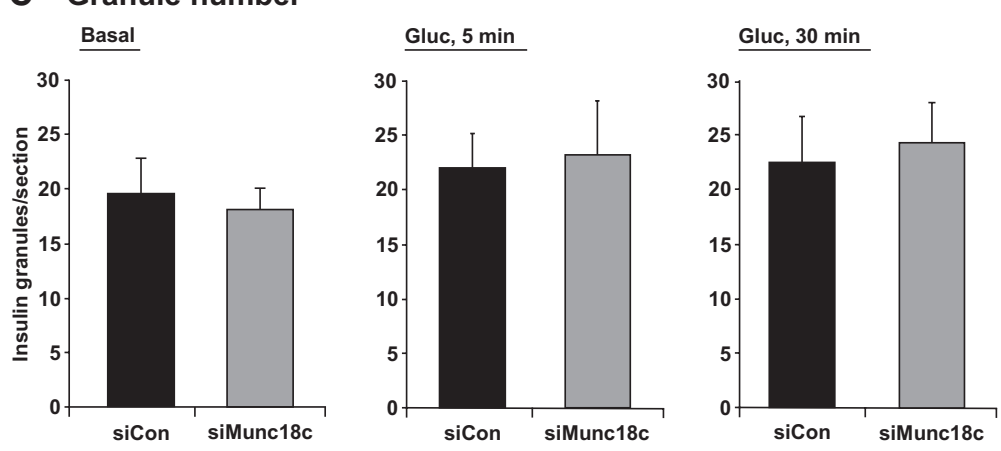

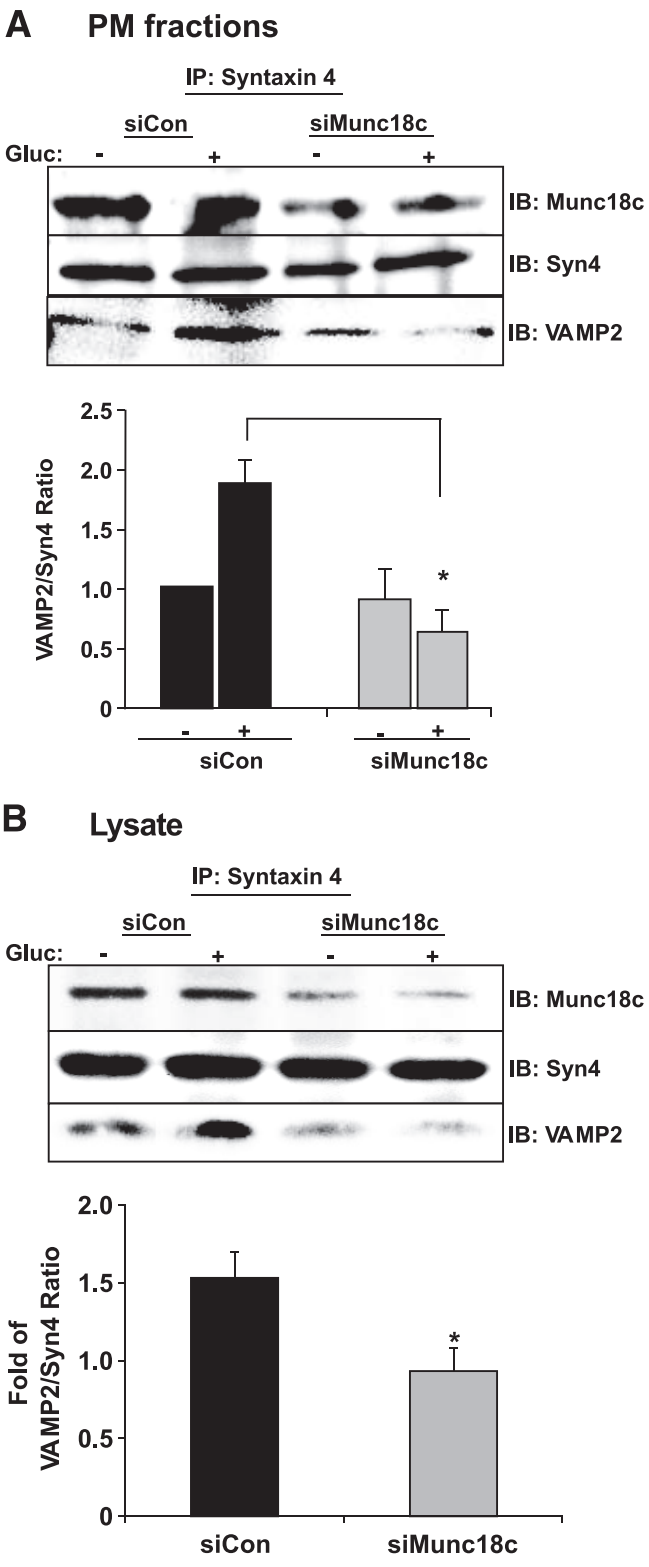

FIG. 6. Munc18c depletion correlates with decreased Syntaxin 4–VAMP2 association. MIN6 cells transduced with siCon-Ad or siMunc18c-Ad were placed in glucose-free MKRBB for 2 h for subsequent stimulation with 20 mmol/l glucose for 5 min and immediately subjected to subcellular fractionation to obtain plasma membrane fractions (*A*) or detergent lysis to obtain cleared detergent cell lysates for subsequent use in anti–Syntaxin 4 immunoprecipitation (IP) reactions (*B*). Immunoprecipitated proteins were resolved on 12% SDS-PAGE for immunodetection of Munc18c, Syntaxin 4 (Syn4), and VAMP2. Data represent the mean ± SE of three to five independent sets of fractions or lysates. *$P < 0.05$ vs. siCon-Ad. Gluc, glucose; IB, immunoblotting.

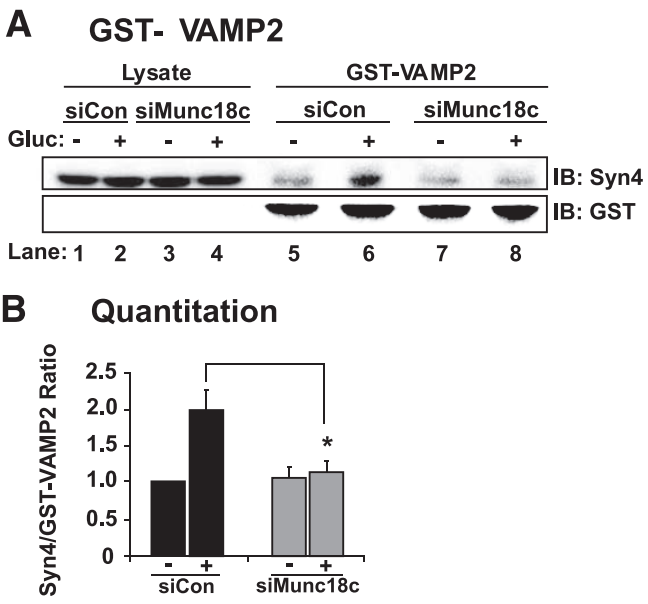

FIG. 7. Depletion of Munc18c decreases Syntaxin 4 accessibility to VAMP2. Detergent cell lysates prepared from MIN6 cells transduced with siCon-Ad or siMunc18c-Ad were incubated with purified GST-VAMP2 linked to beads. GST-VAMP2 and associated proteins were subjected to 12% SDS-PAGE for immunoblotting (IB) with anti–Syntaxin 4 (Syn4) antibody. Anti-GST immunoblotting shows equal loading of GST-VAMP2. Data represent the mean ± SE of five independent sets of lysates (*$P < 0.05$). Gluc, glucose.

DISCUSSION

In a previous study, Munc18c heterozygous (−/+) mouse islets were found to exhibit significantly impaired GSIS under static incubation conditions (29), although the phase affected and the underlying mechanistic defect was undetermined. In this follow-up study, Munc18c protein was found to function selectively in the second phase of GSIS, also referred to as the mobilization phase. In agreement with this finding, our electron microscopy studies revealed a novel requirement for Munc18c in the glucose-mediated mobilization toward/retention of granules at the plasma membrane. Consistent with a role in capture/retention of granules at the plasma membrane, Munc18c was found to be key in facilitating the glucose-stimulated "activation" of Syntaxin, to increase its accessibility to VAMP2. Taken together, these data suggest new positive roles for Munc18c in predocking events that may underlie its requirement in the second phase of GSIS.

To the best of our knowledge, this is the first report to differentiate the need for an SM protein such as Munc18c in Syntaxin 4 accessibility, a step we refer to as "Syntaxin 4 activation," from other steps such as vesicle capture (tethering)/docking/fusion. For example, it has recently been shown that depletion of the Munc18a isoform from INS-1 cells reduces both GSIS and KCl-stimulated secretion from INS-1 cells coordinate with reducing the number of granules present in the total internal reflection fluorescent microscopy (TIRFM) zone at the plasma membrane. Based on this, it was concluded that the role of Munc18a was in vesicle tethering/docking. Similarly, both Munc18a and the nematode SM protein unc-18 are labeled as docking factors, since their depletion from their respective cell types reduced the number of docked release-ready vesicles at the plasma membrane (37–39). Interestingly, the SM protein Vps45 was shown to be required for t-SNARE participation in SNARE complexes (40), but as

with all of the aforementioned studies, this could not be distinguished from effects upon mobilization. Given that the only role for SM proteins to date is related to their rich abundance at the plasma membrane (to which they associate in large part due to their high-affinity binding to their cognate Syntaxin partners), declaring the role(s) of the SM proteins to be at the plasma membrane is reasonable. Our data are consistent with these examples, but clearly distinguished this new mechanistic role for Munc18c in Syntaxin 4 activation in particular because the assay used was not confounded by differential granule abundance at the plasma membrane.

Even with our demonstration for a clearly defined role for Munc18c at the plasma membrane in Syntaxin 4 activation, there are several reasons why Munc18c may also be involved in granule mobilization. First, ~50% of cellular Munc18c resides in the cytosolic compartment in the absence of Syntaxin 4, yet its function in this compartment remains unknown (8). Second, the exocytosis events in which Munc18c is required, i.e., second-phase GSIS and insulin-stimulated GLUT4 vesicle translocation, are relatively slow and sustained events compared with the rapid synaptic vesicle exocytosis and first-phase insulin release events that require Munc18a. Third, second-phase GSIS and insulin-stimulated GLUT4 vesicle translocation involve relatively long-distance granule mobilization events, compared with the short-range docked-primed transition event or the docking of granules already present in the plasma membrane–localized readily releasable pool to support first-phase insulin release or rapid neurotransmitter release. Fourth, Munc18c depletion failed to affect granule distribution in unstimulated cells, consistent with its lack of effect on first-phase secretion, which has been shown to be supported by the release of granules from the readily releasable pool at the plasma membrane (18). Our electron microscopy studies revealed that in Munc18c-depleted cells, the majority of granules remained furthest from the plasma membrane after either 5 or 30 min of glucose stimulation, rather than showing enrichment in the 50- to 300-nm pool. While it is intriguing to suggest that granules were not mobilized from the deeper storage pools of the cell, one cannot exclude testing the possibility that in the absence of adequate Munc18c levels at the plasma membrane, granules mobilized to the plasma membrane then "bounced" and reentered the more distal granule storage pools. Indeed, a reduced retention time of vesicles was noted in Munc18a null chromaffin cells (41).

Although Syntaxin 1A is required for only one phase of insulin release (17), Syntaxin 4 facilitates both phases of insulin secretion (8), and, as such, we had initially predicted that Munc18c would also be required for both phases. This discrepancy could be explained in two ways: *1*) first-phase secretion is elicited from predocked granules, so the need for Syntaxin 4 activation or granule mobilization was alleviated; and *2*) the reminiscent ~25% of Munc18c protein in the Munc18c (−/+) + siMunc18c-Ad islets was sufficient to activate that quotient of Syntaxin 4 required for the first phase, since exocytotic events of first phase are shared with Syntaxin 1 and its cognate Munc18a protein. Whereas the second possibility will require a β-cell–specific null Munc18c knockout model to obtain nearly full Munc18c depletion to assess its requirement in first-phase insulin release, the first possibility mentioned above is certainly compatible with the current concept of vesicle docking.

Other proposed mechanisms for SM proteins have included chaperoning Syntaxin to the plasma membrane (40) as well as in bridging Syntaxin-VAMP2 interactions directly. However, our data here showed that Syntaxin 4 abundance at the plasma membrane was unimpaired in cells depleted of Munc18c, and we and others have previously shown that heteromeric Munc18c-Syntaxin 4–VAMP2 complexes are undetectable in cell and tissue lysates (34,42). Nevertheless, the studies presented here aimed to test the proposed mechanism for SM proteins in transitioning their cognate syntaxins to an "open" state that is more accessible to the other SNARE proteins to promote SNARE core complex assembly (rev. in 23). The present studies support this model, which we and others have proposed to involve stimulus (glucose)-induced tyrosine phosphorylation of Munc18c and additional participation of non-SNARE factors to elicit transient conformational changes in Syntaxin 4 (32,34,43,44).

Factors such as Doc2β, RalA-GTPase, and Munc13-1 have been implicated in biphasic insulin release. For example, RalA depletion in mouse β-cells inhibited both phases of insulin release, attributed to insufficient readily releasable pool size as well as defective granule mobilization to support second-phase exocytosis (45). Munc13-1 was shown to be required for the sustained release of insulin upon prolonged stimulation (46). Munc13-1 can bind to a discrete NH_2-terminal domain of Doc2β, and Doc2β can bind to Munc18a and Munc18c through its C2A and C2B domains, respectively (47,48). In islet β-cells, Doc2β preferentially binds to the tyrosine-phosphorylated form of Munc18c (34). Furthermore, glucose-stimulated tyrosine phosphorylation of Munc18c correlates with its transient dissociation from Syntaxin 4 (32), although whether this transient dissociation induces the conformational change in Syntaxin 4 to increase accessibility to VAMP2 remains to be determined. Lastly, serine/threonine phosphorylation of Munc18c has also been shown to induce dissociation of Munc18c from Syntaxin 4 in pancreatic acinar cells (49), and this is somewhat analogous to the protein kinase C–induced serine/threonine phosphorylation of Munc18a and its dissociation from Syntaxin 1A (50). Given these findings for Munc18a and those presented here for Munc18c, future investigations will be required to determine if Munc18a and Munc18c actions work in concert to control biphasic insulin secretion. Given that novel drug targets will be required to improve exocytotic function in islet β-cells and in skeletal muscle cells of type 2 diabetic patients, our data showing conservation of Munc18c function between exocytotic mechanisms in these two tissue types may point to Munc18c or its novel accessory proteins as new and potentially attractive targets.

ACKNOWLEDGMENTS

This work was supported by National Institutes of Health (NIH) grants DK067912 and DK076614 to D.C.T. and the American Heart Association Postdoctoral Fellowship 0720042Z to E.O.

No potential conflicts of interest relevant to this article were reported.

We thank John Hutton for the gift of MIN6 β-cells and Jenna L. Jewell for providing GST-VAMP2 protein and for critical review of this manuscript. Assistance from the Indiana University School of Medicine Electron Microscopy Center was invaluable.

REFERENCES

1. Ostenson CG, Gaisano H, Sheu L, et al. Impaired gene and protein expression of exocytotic soluble *N*-ethylmaleimide attachment protein receptor complex proteins in pancreatic islets of type 2 diabetic patients. Diabetes 2006;55:435–440
2. Tsunoda K, Sanke T, Nakagawa T, et al. Single nucleotide polymorphism (D68D, T to C) in the syntaxin 1A gene correlates to age at onset and insulin requirement in type II diabetic patients. Diabetologia 2001;44:2092–2097
3. Romeo S, Sentinelli F, Cavallo MG, et al. Search for genetic variants of the SYNTAXIN 1A (STX1A) gene: the −352 A>T variant in the STX1A promoter associates with impaired glucose metabolism in an Italian obese population. Int J Obes (Lond) 2008;32:413–420
4. Bergman BC, Cornier MA, Horton TJ, et al. Skeletal muscle munc18c and syntaxin 4 in human obesity. Nutr Metab (Lond) 2008;5:21
5. Thurmond DC: Regulation of insulin action and insulin secretion by SNARE-mediated vesicle exocytosis. In *Mechanisms of Insulin Action.* Saltiel AR and Pessin JE, Eds. Georgetown, TX, Landes Bioscience, 2007, p. 52–70
6. Yechoor VK, Patti ME, Ueki K, et al. Distinct pathways of insulin-regulated versus diabetes-regulated gene expression: an in vivo analysis in MIRKO mice. Proc Natl Acad Sci U S A 2004;101:16525–16530
7. Spurlin BA, Park SY, Nevins AK, et al. Syntaxin 4 transgenic mice exhibit enhanced insulin-mediated glucose uptake in skeletal muscle. Diabetes 2004;53:2223–2231
8. Spurlin BA, Thurmond DC. Syntaxin 4 facilitates biphasic glucose-stimulated insulin secretion from pancreatic beta-cells. Mol Endocrinol 2006;20:183–193
9. Nagamatsu S, Nakamichi Y, Yamamura C, et al. Decreased expression of t-SNARE, syntaxin 1, and SNAP-25 in pancreatic β-cells is involved in impaired insulin secretion from diabetic GK rat islets: restoration of decreased t-SNARE proteins improves impaired insulin secretion. Diabetes 1999;48:2367–2373
10. Spurlin BA, Thomas RM, Nevins AK, et al. Insulin resistance in tetracycline-repressible Munc18c transgenic mice. Diabetes 2003;52:1910–1917
11. Khan AH, Thurmond DC, Yang C, et al. Munc18c regulates insulin-stimulated glut4 translocation to the transverse tubules in skeletal muscle. J Biol Chem 2001;276:4063–4069
12. Rhodes CJ: Processing of the insulin molecule. In *Diabetes Mellitus: A Fundamental and Clinical Text.* LeRoith T, Olefsky, Eds. Philadelphia, PA, Lippincott Williams & Wilkins, 2000, p. 20–38
13. Meglasson MD, Matschinsky FM. Pancreatic islet glucose metabolism and regulation of insulin secretion. Diabete Metab Rev 1986;2:163–214
14. Satin LS, Cook DL. Voltage-gated Ca2+ current in pancreatic B-cells. Pflugers Arch 1985;404:385–387
15. Cook DL, Hales CN. Intracellular ATP directly blocks K+ channels in pancreatic B-cells. Nature 1984;311:271–273
16. Wiser O, Bennett MK, Atlas D. Functional interaction of syntaxin and SNAP-25 with voltage-sensitive L- and N-type Ca2+ channels. EMBO J 1996;15:4100–4110
17. Ohara-Imaizumi M, Fujiwara T, Nakamichi Y, et al. Imaging analysis reveals mechanistic differences between first- and second-phase insulin exocytosis. J Cell Biol 2007;177:695–705
18. Barg S, Eliasson L, Renstrom E, et al. A subset of 50 secretory granules in close contact with L-type Ca2+ channels accounts for first-phase insulin secretion in mouse β-cells. Diabetes 2002;51 (Suppl. 1):S74–S82
19. Henquin JC, Nenquin M, Stiernet P, et al. In vivo and in vitro glucose-induced biphasic insulin secretion in the mouse: pattern and role of cytoplasmic Ca2+ and amplification signals in β-cells. Diabetes 2006;55:441–451
20. Henquin JC, Dufrane D, Nenquin M. Nutrient control of insulin secretion in isolated normal human islets. Diabetes 2006;55:3470–3477
21. Nunemaker CS, Wasserman DH, McGuinness OP, et al. Insulin secretion in the conscious mouse is biphasic and pulsatile. Am J Physiol Endocrinol Metab 2006;290:E523–E529
22. Zawalich WS, Yamazaki H, Zawalich KC. Biphasic insulin secretion from freshly isolated or cultured, perifused rodent islets: comparative studies with rats and mice. Metabolism 2008;57:30–39
23. Jahn R, Scheller RH. SNAREs: engines for membrane fusion. Nat Rev Mol Cell Biol 2006;7:631–643
24. Garcia EP, Gatti E, Butler M, et al. A rat brain Sec1 homologue related to Rop and UNC18 interacts with syntaxin. Proc Natl Acad Sci U S A 1994;91:2003–2007
25. Tellam JT, McIntosh S, James DE. Molecular identification of two novel Munc-18 isoforms expressed in non-neuronal tissues. J Biol Chem 1995;270:5857–5863
26. Tellam JT, Macaulay SL, McIntosh S, et al. Characterization of Munc-18c and syntaxin-4 in 3T3–L1 adipocytes: putative role in insulin-dependent movement of GLUT-4. J Biol Chem 1997;272:6179–6186
27. Tamori Y, Kawanishi M, Niki T, et al. Inhibition of insulin-induced GLUT4 translocation by Munc18c through interaction with syntaxin4 in 3T3–L1 adipocytes. J Biol Chem 1998;273:19740–19746
28. Tomas A, Meda P, Regazzi R, et al. Munc 18–1 and granuphilin collaborate during insulin granule exocytosis. Traffic 2008;9:813–832
29. Oh E, Spurlin BA, Pessin JE, et al. Munc18c heterozygous knockout mice display increased susceptibility for severe glucose intolerance. Diabetes 2005;54:638–647
30. Thurmond DC, Ceresa BP, Okada S, et al. Regulation of insulin-stimulated GLUT4 translocation by Munc18c in 3T3L1 adipocytes. J Biol Chem 1998;273:33876–33883
31. Nevins AK, Thurmond DC. Caveolin-1 functions as a novel Cdc42 guanine nucleotide dissociation inhibitor in pancreatic beta-cells. J Biol Chem 2006;281:18961–18972
32. Oh E, Thurmond DC. The stimulus-induced tyrosine phosphorylation of Munc18c facilitates vesicle exocytosis. J Biol Chem 2006;281:17624–17634
33. Nevins AK, Thurmond DC. A direct interaction between Cdc42 and vesicle-associated membrane protein 2 regulates SNARE-dependent insulin exocytosis. J Biol Chem 2005;280:1944–1952
34. Jewell JL, Oh E, Bennett SM, et al. The tyrosine phosphorylation of Munc18c induces a switch in binding specificity from Syntaxin 4 to Doc2beta. J Biol Chem 2008;283:21734–21746
35. Preitner F, Ibberson M, Franklin I, et al. Gluco-incretins control insulin secretion at multiple levels as revealed in mice lacking GLP-1 and GIP receptors. J Clin Invest 2004;113:635–645
36. Kanda H, Tamori Y, Shinoda H, et al. Adipocytes from Munc18c-null mice show increased sensitivity to insulin-stimulated GLUT4 externalization. J Clin Invest 2005;115:291–301
37. Voets T, Toonen RF, Brian EC, et al. Munc18–1 promotes large dense-core vesicle docking. Neuron 2001;31:581–591
38. Toonen RF, Wierda K, Sons MS, et al. Munc18–1 expression levels control synapse recovery by regulating readily releasable pool size. Proc Natl Acad Sci U S A 2006;103:18332–18337
39. Weimer RM, Richmond JE, Davis WS, et al. Defects in synaptic vesicle docking in unc-18 mutants. Nat Neurosci 2003;6:1023–1030
40. Bryant NJ, James DE. Vps45p stabilizes the syntaxin homologue Tlg2p and positively regulates SNARE complex formation. EMBO J 2001;20:3380–3388
41. Toonen RF, Kochubey O, de Wit H, et al. Dissecting docking and tethering of secretory vesicles at the target membrane. EMBO J 2006;25:3725–3737
42. Latham CF, Lopez JA, Hu SH, et al. Molecular dissection of the Munc18c/syntaxin4 interaction: implications for regulation of membrane trafficking. Traffic 2006;7:1408–1419
43. Hu SH, Latham CF, Gee CL, et al. Structure of the Munc18c/Syntaxin4 N-peptide complex defines universal features of the N-peptide binding mode of Sec1/Munc18 proteins. Proc Natl Acad Sci U S A 2007;104:8773–8778
44. Schmelzle K, Kane S, Gridley S, et al. Temporal dynamics of tyrosine phosphorylation in insulin signaling. Diabetes 2006;55:2171–2179
45. Lopez JA, Kwan EP, Xie L, et al. The RalA GTPase is a central regulator of insulin exocytosis from pancreatic islet beta cells. J Biol Chem 2008;283:17939–17945
46. Kang L, He Z, Xu P, et al. Munc13-1 is required for the sustained release of insulin from pancreatic beta cells. Cell Metab 2006;3:463–468
47. Verhage M, de Vries KJ, Roshol H, et al. DOC2 proteins in rat brain: complementary distribution and proposed function as vesicular adapter proteins in early stages of secretion. Neuron 1997;18:453–461
48. Ke B, Oh E, Thurmond DC. Doc2beta is a novel Munc18c-interacting partner and positive effector of syntaxin 4-mediated exocytosis. J Biol Chem 2007;282:21786–21797
49. Cosen-Binker LI, Lam PP, Binker MG, et al. Alcohol/cholecystokinin-evoked pancreatic acinar basolateral exocytosis is mediated by protein kinase C alpha phosphorylation of Munc18c. J Biol Chem 2007;282:13047–13058
50. Fujita Y, Sasaki T, Fukui K, et al. Phosphorylation of Munc-18/n-Sec1/rbSec1 by protein kinase C: its implication in regulating the interaction of Munc-18/n-Sec1/rbSec1 with syntaxin. J Biol Chem 1996;271:7265–7268